Journal of Power Sources 196 (2011) 6595–6602

Contents lists available at ScienceDirect

Journal of Power Sources

journal homepage: www.elsevier.com/locate/jpowsour

Efficient quantum dot-sensitized solar cell with polystyrene-modified TiO_2 photoanode and with guanidine thiocyanate in its polysulfide electrolyte

Chen-Yu Chou[a], Chuan-Pei Lee[a], R. Vittal[a], Kuo-Chuan Ho[a,b,*]

[a] Department of Chemical Engineering, National Taiwan University, Taipei 10617, Taiwan
[b] Institute of Polymer Science and Engineering, National Taiwan University, Taipei 10617, Taiwan

ARTICLE INFO

Article history:
Received 25 November 2010
Received in revised form 25 March 2011
Accepted 29 March 2011
Available online 5 April 2011

Keywords:
Guanidine thiocyanate (GuSCN)
Monodispersed polystyrene (PS)
Polysulfide electrolyte
Quantum dot-sensitized solar cell (QDSSC)
Successive ionic layer adsorption and reaction (SILAR)

ABSTRACT

Monodispersed polystyrene (PS, *ca.* 300 nm) latex particles are incorporated into a TiO_2 film. A polystyrene-modified TiO_2 film (M-TiO_2) with micro-cluster structure, containing micro/nano-composite pores is thus obtained after sintering. Cadmium sulfide (CdS) quantum dots (CdS-QDs) are accumulated over M-TiO_2 and bare TiO_2 films (B-TiO_2) by successive ionic layer adsorption and reaction (SILAR); we designate these films as M-TiO_2/CdS and B-TiO_2/CdS, respectively. Influence of SILAR cycles used for depositing CdS on B-TiO_2 and M-TiO_2 films on the performance of the pertinent quantum dot-sensitized solar cells (QDSSCs) is studied. The QDSSC with 6 SILAR cycles of M-TiO_2/CdS (M-TiO_2/CdS6) exhibited a solar-to-electricity conversion efficiency (η) of 1.79%, while the cell with B-TiO_2/CdS5 shows an η of 1.35%, under the illumination of one sun. Moreover, guanidine thiocyanate (GuSCN) is found to be a promising additive to the polysulfide electrolyte. The additive renders higher conversion efficiency (2.01%) to its QDSSC. Durability of the CdS-QDSSC is also tested. Scanning electron microscopy (SEM) is used to obtain the images of TiO_2 films and energy-dispersive X-ray spectroscopy (EDX) is employed to study the stoichiometric ratios of M-TiO_2/CdS and B-TiO_2/CdS. Incident photon-to-current conversion efficiencies (IPCE) of the QDSSCs are obtained to confirm the J_{SC} behaviors of the cells.

1. Introduction

Since the inception of intensive research on dye-sensitized solar cells (DSSCs) by Michael Grätzel and his co-workers in 1991, the cells have attracted a lot of attention, attributable to their low cost and relatively high energy conversion efficiency [1,2]. Extensive research has been carried out on designing and testing of a variety of organoinorganic and organic dye molecules, intending to improve both the efficiency and the stability of the DSSCs [3–5]. Ru-complex dyes were established to be the best sensitizers for DSSCs with an electrolyte containing iodide/triiodide redox system [6]. Inorganic semiconductor nanocrystals, or the so-called quantum dots (QDs), have also been considered, along with several dye molecules, for solar cells as attractive light harvesters, and the pertinent cells are called quantum dot-sensitized solar cells (QDSSCs). There are many kinds of QDs that absorb visible light, e.g., CdS [7–11], CdSe [12–15], PbS [16], InP [17], InAs [18], and ZnSe [19]. CdS and CdTe have been widely used as main materials in thin film solar cells (TFSCs). There has been, however, a concern about the environmental safety of the usage of heavy metals like Cd in QDSSCs. In order to ensure the safety and avoid the damage to the environment, some TSFC companies, e.g., First Solar®, have announced an insurance policy in 2005 to fund solar module reclamation and recycling expenses at the end of utilization of the product. This recycle mechanism has been soon accepted by several countries, e.g., US and Germany. Besides, thanks to the advancements in the technology on the assemblage of the cells and to the stable property of cadmium compounds, cadmium was capsulated in the solar cell modules, where it was inevitable; this technique has been believed to be safe for health and environment. QDs have several important properties and advantages that are different from those of conventional organic or organoinorganic dyes. For instance, QDs have higher extinction coefficients [20] and better heat resistance compared to those of molecular dyes; their absorption spectrum can be tuned via size-dependent bandgaps, arising from quantum confinement effect [21]. One more potential advantage of quantum dots is their multiple exciton generation (MEG) [22], that is generation of multiple electron–hole (e^-–h^+) pairs per photon; the absorbed photon energy above the semiconductor QDs bandgap may be utilized to generate another e^-–h^+ pair. The maximum theoretical conversion efficiency of a p–n junction solar cell, assuming a p–n junction band gap of 1.1 V, was calculated by Shockley and Queisser [23] and is about 31%. The multiple exciton generation, as men-

* Corresponding author at: Department of Chemical Engineering, National Taiwan University, Taipei 10617, Taiwan. Tel.: +886 2 2366 0739; fax: +886 2 2362 3040.
E-mail address: kcho@ntu.edu.tw (K.-C. Ho).

0378-7753/$ – see front matter © 2011 Elsevier B.V. All rights reserved.
doi:10.1016/j.jpowsour.2011.03.084

tioned above, could break one of the constraints in Shockley and Queisser limit and could lead theoretically to a solar-to-electricity conversion efficiency of about 66% in the limit of an infinite stack of band gaps perfectly matched to the solar spectrum in a tandem cell [22]. Crystalline silicon devices (p–n junction) are now approaching the theoretical limiting efficiency of 31%.

Despite these powerful merits of QD materials, the power conversion efficiency of a QDSSC is still low with reference to that of a DSSC (maximum achieved efficiency for a DSSC is little more 11%). The efficiency achieved in the case of most of the reports on CdS-QDSSCs is about 1–2%. Lee and Chang [7] reported a conversion efficiency of 1.15% for a CdS-QDSSC with a polysulfide electrolyte. Shalom et al. [11] have obtained an efficiency of 1.24% for a similar CdS-QDSSC, using an amorphous TiO_2 coating. Zhang et al. have obtained an efficiency of 1.47% by employing a carbon electrode as the counter electrode in a CdS-QDSSC [24]. One of the reasons for the low efficiencies is the difficulty pertaining to the charge transfer process in the semiconductor film and to the collection of this charge at the substrate of the photoanode. Discussions in detail about the kinetics of QDs and comparisons of DSSCs with QDSSCs could be found in the certain literatures [25,26]. On the other hand, the difficulty in obtaining a well-covered QDs layer on the TiO_2 crystalline surface is also a reason for the poor performance of a QDSSC. Several approaches have been made to connect compactly QDs and nanocrystalline TiO_2, by taking advantages of solution based chemical bath deposition (CBD) [13,18,27] and successive ionic layer adsorption and reaction (SILAR) [10,15], or using bifunctional linkers [12].

Another important issue concerns the electrolytes of the QDSSCs. Unfortunately, commonly used I^-/I_3^- redox couple that acts quite well in DSSCs, is highly corrosive to most of the semiconductor QDs. For this reason, finding an appropriate, non-corrosive electrolyte is very important. One attractive electrolyte with notable stability for a liquid junction QDSSC is polysulfide electrolyte with the redox couple, S^{2-}/S_x^{2-} [7,12,28,29]; yet its composition has not been fully explored. The corresponding fill factor (*FF*) is relatively lower than that obtainable when an iodide/triiodide electrolyte is employed.

In our previous work, we have reported that a micro-porous structure of TiO_2 film in a DSSC could reduce the ionic resistance in the film for a gel polymer electrolyte [30]. Herein, we extend this concept and deliver a simple way to construct a micro/nano-composite porous structure for a TiO_2 film, intending to reduce the ionic diffusion resistance in the TiO_2 electrode, to obtain an uniform CdS QDs deposition on and in the TiO_2 film, and to avoid the unfavourable clogging of pores. We also demonstrate the improvement of the polysulfide electrolyte in terms of cell efficiency, by incorporating guanidine thiocyanate (GuSCN) in the electrolyte. The cell with GuSCN in this study shows an efficient efficiency of 2.01% at full sun intensity. This is the first study to use polystyrene-modified TiO_2 film for preparing the photoanode of a QDSSC. The EDX study for different SILAR cycles is also a novel aspect of this report. The report establishes for the first time that GuSCN as an additive in the polysulfide electrolyte of a QDSSC can enhance the cell efficiency considerably.

2. Experimental

2.1. Materials

Cadmium nitrate ($Cd(NO_3)_2{\cdot}4H_2O$, ≧99%), polystyrene solution (10 wt.% PS latex particles in H_2O, 0.3 μm average diameter), sodium sulfide ($Na_2S{\cdot}9H_2O$, ≧98%), sulfur (S), potassium chloride (KCl, ≧99%), guanidine thiocyanate (GuSCN, 99%), Ti(IV) tetraisopropoxide (TTIP, ≧98%), acetylacetone (AA, 99.5%), Triton X®-100 (>99.95%), ethanol (99.8%), methanol (99.8%), isopropyl alcohol (IPA, 99.5%), and silica (SiO_2, 12 nm, 99.8%) were obtained from Aldrich.

2.2. Preparation of photoanodes for QDSSCs and the corresponding SILAR process

Commercial TiO_2 powder (P25, Degussa, 7.5 g) was slowly added into a solution containing AA (1 ml) and DI-water (9 g) and the contents were thoroughly mixed and stirred for 3 days; 250 μL of Triton® X-100 was then added to the well-dispersed colloidal solution. The final mixture was stirred for additional 2 days to obtain a bare TiO_2 paste. For the desired polystyrene (PS)-modified TiO_2 paste, the procedure was the same as above except for adding monodispersed PS solution into the solution (AA and DI-water) before the addition of TiO_2 powder and Triton® X-100; the thus obtained paste has 8 wt.% of PS in the final colloidal solution.

A fluorine-doped SnO_2 (FTO, TEC-7, 7 Ω sq.$^{-1}$, transmittance ≧80%, NSG America, Inc., NJ, USA) and a tin-doped In_2O_3 (ITO, 7 Ω sq.$^{-1}$, Ritek Corporation, Hsinchu, Taiwan) conducting glasses were first cleaned with a neutral cleaner and then washed with DI-water, acetone, and IPA sequentially. The conducting surface of the FTO was treated with a solution of TTIP (0.028 g) in ethanol (10 ml) for obtaining a good mechanical contact between the conducting glass and the TiO_2 film, as well as for isolating the conducting glass surface from the electrolyte. A 10 μm-thick film of TiO_2 with PS particles was coated on the treated FTO glass by spin coating method, and a portion of 0.4 cm × 0.4 cm was selected from it for active area by removing the side portions by scrapping. The TiO_2 film was gradually heated to 450 °C in an oxygen atmosphere, and subsequently sintered at that temperature for 30 min to remove the surfactant (Triton® X-100) and to burn out the PS latex particles, and thereby to form large pores in the TiO_2 film. A reference TiO_2 film was also obtained in a similar way, however, without the use of polystyrene during its preparation. We designate this film as bare TiO_2 film (B-TiO_2). The morphologies of bare TiO_2 film (B-TiO_2) and PS-modified TiO_2 film (M-TiO_2), i.e., TiO_2 film obtained using PS during the preparation of its paste, were observed from the images of scanning electron microscopy (SEM, Nova NanoSEM 230, FEI).

The prepared B-TiO_2 and M-TiO_2 electrodes were dipped into 0.4 M $Cd(NO_3)_2$ in ethanol for 5 min, rinsed by pure ethanol, dried with N_2, dipped into 0.4 M Na_2S in methanol for 5 min, and then rinsed by pure methanol, dried with N_2. This procedure is termed as 1 SILAR cycle. Different SILAR cycles were performed until the desired photoanodes were achieved. The elemental contents of the deposited metal chalcogenide in different conditions of photoanodes and also at different depths beneath the film were determined by energy dispersive X-ray (EDX) spectra, equipped with SEM under cross-sectional view.

2.3. Assembly of the QDSSCs

The thus prepared TiO_2/CdS electrode was placed on the gold-sputtered conducting glass electrode (ITO/Au) to fabricate the full cell. The two electrodes were separated by a 25 μm-thick surlyn® (SX1170-25, Solaronix S.A., Aubonne, Switzerland) and sealed by heating. A solution consisting of Na_2S (0.5 M), S (2.0 M), and KCl (0.2 M) in methanol/water (7:3 by volume) was used as the electrolyte [7]. Two more kinds of other polysulfide electrolytes containing GuSCN (0.1 M) or SiO_2 (1.0 wt.%) were also prepared. The electrolyte was injected into the gap between the electrodes by capillarity; during the fixing of the surlyn® tape a small gap was left at the edges of the electrodes; this gap was used for injecting

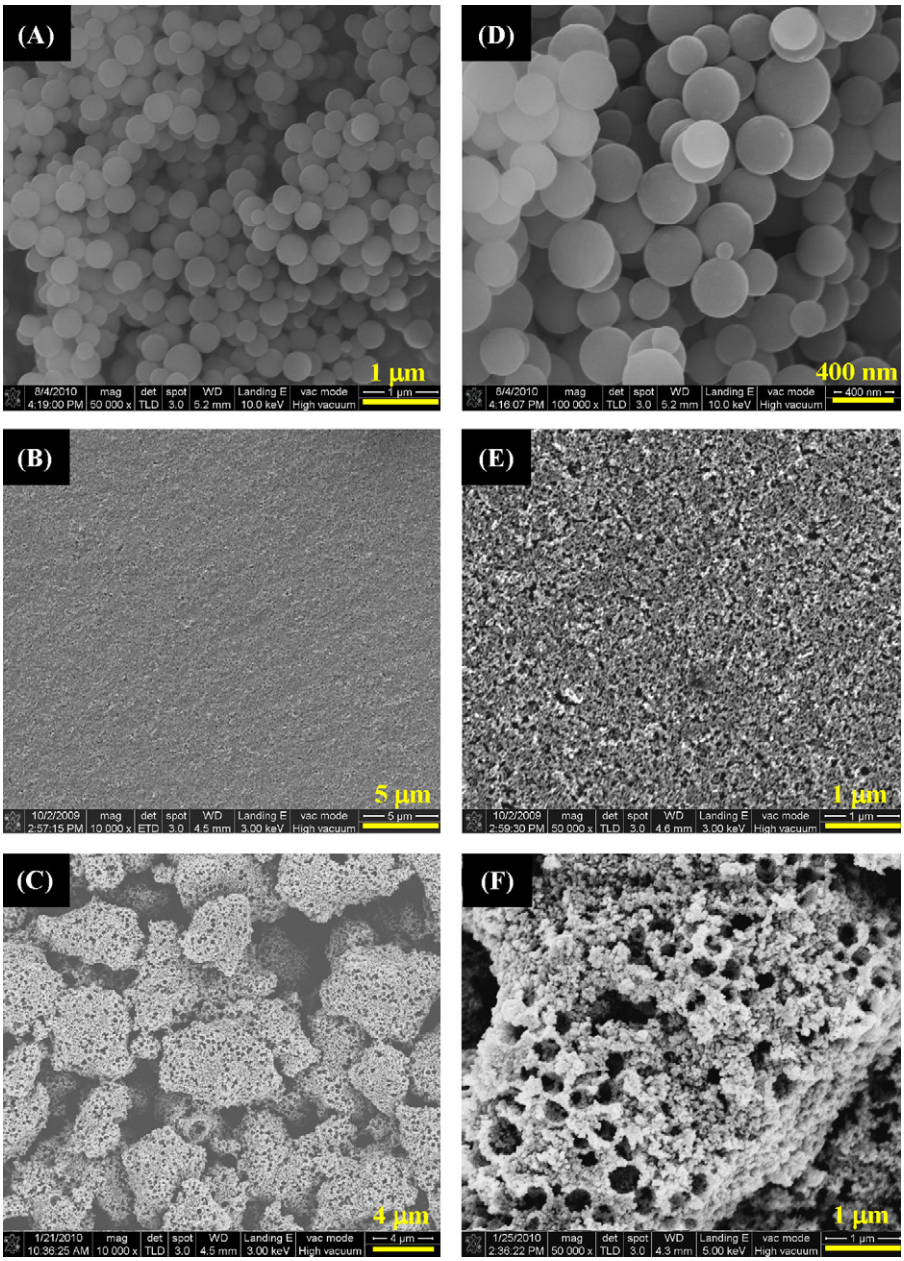

Fig. 1. SEM images of (A) PS particles, (B) B-TiO_2 film, and (C) M-TiO_2 film; (D), (E), and (F) are corresponding images of (A), (B), and (C), respectively, at higher magnification.

the electrolyte, and the gap was sealed with hot-melt glue after the injection of the electrolyte.

2.4. Instrumentation

The surface of the QDSSC was illuminated by a class A quality solar simulator (PEC-L11, AM1.5G, Peccell Technologies, Inc.), and the incident light intensity (100 mW cm^{-2}) was calibrated with a standard Si cell (PECSI01, Peccell Technologies, Inc.). The photoelectrochemical characteristics of the QDSSCs were recorded with a potentiostat/galvanostat (PGSTAT 30, Autolab, Eco-Chemie, the Netherlands). Morphologies of PS particles, and different TiO_2 films were observed using a scanning electron microscope (SEM, Nova NanoSEM 230, FEI Ultra-High Resolution FE-SEM with low vacuum mode); elemental analysis of TiO_2 films covered with CdS was made with the same SEM, equipped with a mode for *in situ* energy dispersive X-ray (EDX) spectra. Incident photons-to-current conversion efficiency (IPCE) curves were obtained at short-circuit condition. The light source was a 450 W Xe lamp (Oriel Instrument, model 6266) equipped with a water-based IR filter (Oriel Instrument, model 6123NS); light was focused through a monochromator (Oriel Instrument, model 74100) onto the photovoltaic cell. The monochromator was incremented through the visible spectrum to generate the IPCE (λ). The equation and parameters used for calculating IPCE values (λ) were the same as reported in the previous literatures [31].

3. Results and discussion

3.1. SEM analyses of polystyrene particles, bare TiO_2 film, and modified TiO_2 film

We intended to obtain a well-covered, uniform CdS layer on a structure-designed TiO_2 film for making an efficient photoanode and ultimately its QDSSC [15,32]. We expected that a micro/nano-composited porous TiO_2 structure would have good permeability

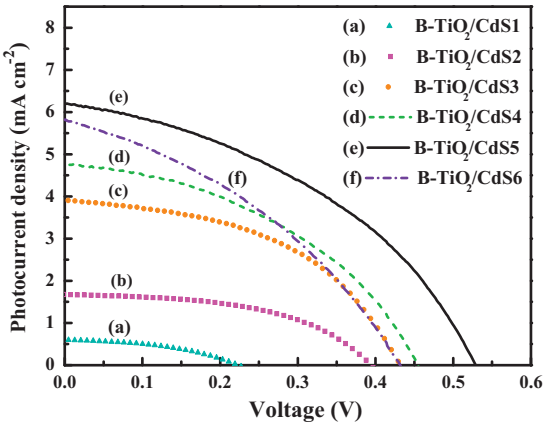

Fig. 2. *I–V* curves of QDSSCs with various bare TiO_2 films (B-TiO_2) obtained using 1–6 SILAR cycles for depositing CdS on them; the measurements were made at 100 mW cm^{-2}.

and would enable a better SILAR process for the whole film. In order to obtain this type of structure, we incorporated into a bare TiO_2 film monodispersed polystyrene (PS), which is an aromatic polymer commonly used as latex particles. Fig. 1 shows top view scanning electron microscopic (SEM) images of commercial PS particles, B-TiO_2 film, and M-TiO_2 film, at two magnifications. The commercial PS particles with an average size of 300 nm are shown in Fig. 1A and D. It can be seen that the B-TiO_2 film (Fig. 1B and E) is dense with an average pore size of about 100 nm. When the PS particles were burned out from the modified TiO_2 film by sintering the film at 450 °C, a micro/nano-composited porous TiO_2 film (M-TiO_2) with an average pore size of about 300 nm (consistent with PS particle size) was formed (Fig. 1C and F). This structure-designed TiO_2 film consisted of not only micro size pores caused by TiO_2 clusters but also nano size pores caused by PS latex particles. As can be compared in Fig. 1E and F, the pore size of B-TiO_2 film is much smaller than that of M-TiO_2 film. CdS-QDs were first deposited on B-TiO_2 film using a precursor solution containing the cations Cd^{2+} and the anions S^{2-}; this precursor solution was used as the reagent for various SILAR cycles (1–6 cycles). We could observe that the B-TiO_2 films gradually became denser in yellow; this implied a progressive formation of the CdS nanocrystals on the film. B-TiO_2 films were coated with CdS using a number of SILAR cycles as described in Section 2 and the corresponding photoanodes were prepared. QDSSCs were fabricated using these photoanodes and the photoanodes or films were designated as B-TiO_2/CdS1 to B-TiO_2/CdS6, where a number indicates the number of SILAR cycles used for that case.

3.2. Photovoltaic parameters of QDSSCs with B-TiO_2/CdS1 to B-TiO_2/CdS6

I–V characteristics of these QDSSCs were obtained under an illumination of 100 mW cm^{-2}, and are shown in Fig. 2; the corresponding photovoltaic parameters are listed in Table 1. The cell using B-TiO_2/CdS1 as the photoanode shows an efficiency of only 0.06% (Table 1); with the increase of SILAR cycles from 1 to 5, there is a steady increase in the open-circuit voltage (V_{OC}), the short-circuit current density (J_{SC}), and the corresponding overall power conversion efficiency (η) of the QDSSCs. Increasing SILAR cycles leads to increasing amount of CdS particles on the B-TiO_2 film and thereby increasing light-harvesting efficiency; this increasing light-harvesting efficiency renders higher J_{SC}'s to the corresponding cells. The fill factor (*FF*) has increased with 2 SILAR cycles, with reference to that of one SILAR cycle (from 0.43 to 0.50) and then decreased rapidly with each additional SILAR cycle. At one SILAR cycle the quantity of CdS on TiO_2 film is expected to be minimum and thus its light harvesting capacity would be minimum; this naturally leads a low J_{SC}; a low J_{SC} implies low concentration of conduction band electrons in the TiO_2 film which in turn implies low V_{OC}; a low V_{OC} and J_{SC} would render a low *FF* by definition of *FF*. Thus the QDSSC with one SILAR cycle exhibits a minimum *FF* and thereby a minimum efficiency of 0.06%. With two SILAR cycles, the quantity of CdS on TiO_2 film increases thereby increasing the light harvesting efficiency. With the same logic as discussed just now an increased quantity of CdS should render a higher J_{SC}, V_{OC}, *FF*, and η for the pertinent QDSSC; this indeed is the case with 2 SILAR cycles. However, other factors play their role if the thickness of the CdS film increases beyond a limit. When the thickness of CdS increases with 3–6 SILAR cycles, the internal resistance would increase and the *FF* value would decrease, as indeed is the case with SILAR cycles of 3–6. It is also true that the light harvesting efficiency increases with the increase of CdS; this leads to an increase in J_{SC}; increase in J_{SC} implies increase in electric field in the circuit of the cell and thereby increase of V_{OC} of the cell; these explanations support the observation in Table 1 that the values of J_{SC}, V_{OC}, and η show a steady increase with the increase of SILAR number from 1 to 5. The power conversion efficiency decreases with 6 SILAR cycles (0.92%), with reference to that with 5 SILAR cycles (1.35%). The pores among TiO_2 nanoparticles may become smaller with excessive CdS and may thus cause an unfavourable clogging among TiO_2 and CdS particles [32], which would reduce the diffusion of S_x^{2-}/S^{2-} ions into the TiO_2 film; this reduced diffusion results in reduced J_{SC}, V_{OC}, and ultimately reduced η. It may be argued that higher quantity of CdS may be associated with higher light harvesting capacity; it is at the same time true that the upper layer of a multilayered CdS with 6 SILAR cycles may not be in direct contact with TiO_2 film and its electron injection rate to the TiO_2 particles may be retarded; thus this can be another reason for the reduced J_{SC} in the case of 6 SILAR cycles; this situation is also favourable for a decrease in V_{OC}, because in this situation of CdS with 6 SILAR cycles there would be recombination of injected electrons with holes in the TiO_2 particles or with the S_x^{2-} ions of the electrolyte [25]; Table 1 indeed shows a reduced V_{OC} in the case of the cell with 6 SILAR cycles, compared to that in the case of the cell with 5 SILAR cycles.

Table 1
Photovoltaic parameters of QDSSCs with B-TiO_2/CdS obtained using 1–6 SILAR cycles for depositing CdS on them; the measurements were made at 100 mW cm^{-2}.

Photoanode films	V_{OC} (mV)	J_{SC} (mA cm^{-2})	*FF*	η (%)
B-TiO_2/CdS1	223	0.59	0.43	0.06
B-TiO_2/CdS2	397	1.68	0.50	0.33
B-TiO_2/CdS3	434	3.91	0.47	0.81
B-TiO_2/CdS4	453	4.77	0.43	0.92
B-TiO_2/CdS5	529	6.19	0.41	1.35
B-TiO_2/CdS6	431	5.82	0.37	0.92

3.3. SEM analysis of B-TiO_2/CdS5, B-TiO_2/CdS6, and M-TiO_2/CdS6

Fig. 3A shows cross-sectional SEM micrograph of B-TiO_2/CdS5 film, Fig. 3B shows that of B-TiO_2/CdS6 film, and Fig. 3C shows that of M-TiO_2/CdS6 film; A1–A3, B1–B3, and C1–C3 in each SEM image of Fig. 3 are the spots at which *in situ* energy dispersive X-ray (EDX) spectral analyses were made. The thickness of each film in Fig. 3 was maintained to be *ca.* 10 μm. Fig. 3A shows B-TiO_2 film covered with CdS when the latter was deposited using 5 SILAR cycles; the film is porous and the structure is favourable for ion diffusion and electron transfer through the film. Fig. 3B shows B-TiO_2 film with 6 SILAR cycles for CdS deposition; this film has fewer pores and there seems to exist a clogging among TiO_2 and CdS particles. The high J_{SC} in the case of QDSSC with the film in Fig. 3A (Fig. 2 and Table 1) and the low J_{SC} in the case of QDSSC with the film in Fig. 3B (Fig. 2 and

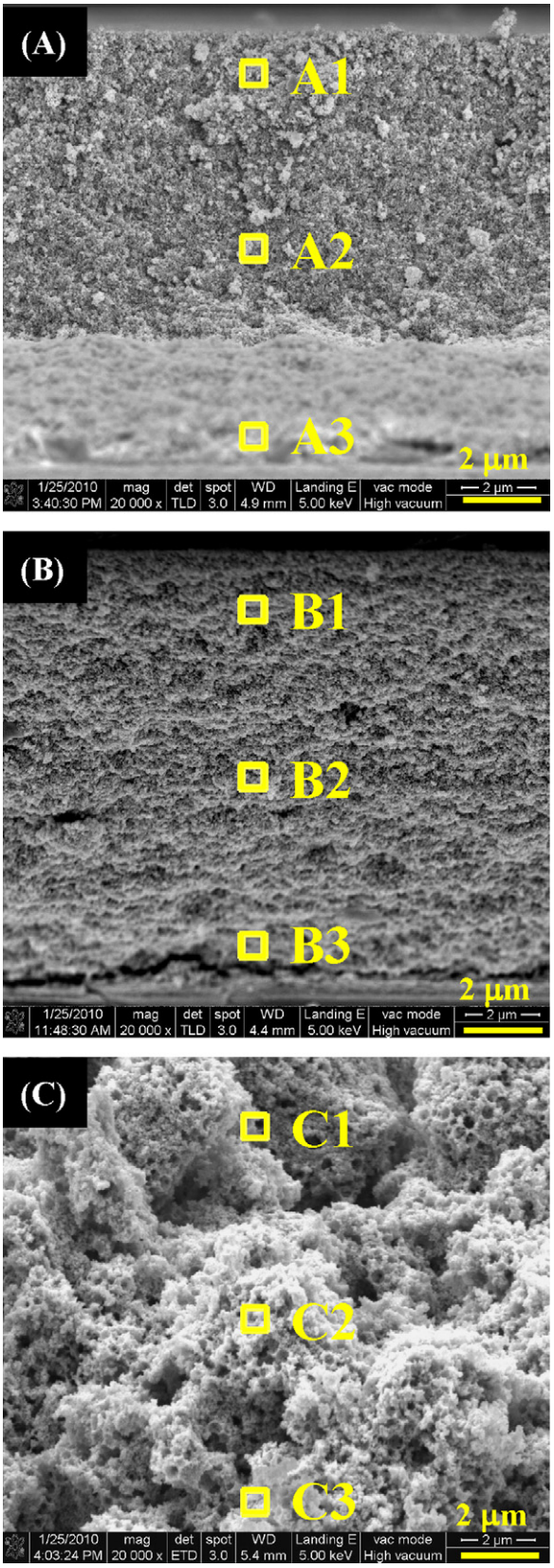

Fig. 3. Cross-sectional SEM images of (A) B-TiO_2 film with 5 SILAR cycles, (B) B-TiO_2 film with 6 SILAR cycles, and (C) M-TiO_2 film with 6 SILAR cycles; A1–A3, B1–B3, and C1–C3 in each SEM image are the spots at which *in situ* energy dispersive X-ray (EDX) spectra analyses were made.

Table 1) are in consistency with these explanations. Fig. 3C shows M-TiO_2 film covered with CdS when the latter was deposited using 6 SILAR cycles. Film in Fig. 3C is completely different from films in Fig. 3A and B. The film in Fig. 3C is very porous in spite of the fact that it is covered with CdS deposited at 6 SILAR cycles. The porous structure in the M-TiO_2 film in Fig. 3C is the result of its prior modification by polystyrene before the application of SILAR cycles for the deposition of CdS. This porous structure is very favourable for uniform deposition of CdS, for ion diffusion and electron transfer through the film. Indeed the QDSSC with M-TiO_2/CdS6 shows much more higher efficiency than that of the cell with B-TiO_2/CdS5, as can be noted in further discussions.

3.4. EDX analysis of B-TiO_2/CdS5, B-TiO_2/CdS6, and M-TiO_2/CdS6

Table 2 shows elemental composition in atomic percentage of the three films in Fig. 3. B-TiO_2/CdS5 (EDX) in Table 2 corresponds to Fig. 3A, B-TiO_2/CdS6 to Fig. 3B and M-TiO_2/CdS6 to Fig. 3C. The Cd/S atomic ratios at different spots (A1, A2, and A3; B1, B2, and B3; C1, C2, and C3) of each film are given at the bottom of the table. The CdS ratios at A1, A2, and A3, i.e., from top to bottom of the film B-TiO_2/CdS5 (case A in Table 2 and Fig. 3A) are 0.71, 0.82, and 0.88, respectively. A Cd/S ratio value of less than 1 could be traced back to the rinsing of the electrode with ethanol during the SILAR process (see Section 2); this rinsing could have removed some of the Cd^{2+} ions after their deposition onto the B-TiO_2 film; although S^{2-} ions were also rinsed with methanol subsequently in the SILAR process (see Section 2), there probability of removal was expected to be quantitatively lesser than that of Cd^{2+} ions; this is because the S^{2-} ions were associated with Cd^{2+} ions existing in the solution for reaction. Thus, the amount of S^{2-} ions rinsed out by solvent could be lesser than that of Cd^{2+} ions; this type of differential removals of S^{2-} ions and Cd^{2+} ions during the SILAR process can cause atomic ratios of Cd/S to be less than 1. These results could be further confirmed by inverse SILAR process, i.e., B-TiO_2 electrodes were dipped first into 0.4 M Na_2S and then into 0.4 M $Cd(NO_3)_2$ in the SILAR process, without changing other treatments. This doping of S^{2-} ions first into the TiO_2 film rendered Cd/S ratios of higher than 1. The Cd/S ratios from top to bottom of the film B-TiO_2/CdS5 were 1.13, 1.04, and 1.07, respectively, in the inverse SILAR process (EDX data are shown in supporting information, Table S1 and Fig. S1). This can be understood better by considering that S^{2-} ions doped into the film in the first SILAR cycle could be washed away by the rinsing of the film with methanol, especially because S^{2-} ions could be repulsed electrostatically by the partial negative charge of the TiO_2 film. Case B (corresponding to film B-TiO_2/CdS6 of Fig. 3B) shows that the Cd/S atomic ratios in the film B-TiO_2/CdS6 increased from top to bottom of the film, i.e., from B1 to B3, and indeed there is a dramatic increase of Cd^{2+} at the bottom of the film. This EDX data illustrate that at the bottom of the B-TiO_2/CdS6 film, the crystal growth of CdS QDs is very uneven and the atomic ratio is far from 1. On the contrary, case C, corresponding to the film M-TiO_2/CdS6 in Fig. 3C does not show this trend of unevenness, and the ratios are 0.85, 0.84, and 0.78 from top to bottom. It can be seen that the stoichiometric ratio between Cd and S throughout the film M-TiO_2/CdS6 is much more even than that in the case of the film B-TiO_2/CdS6.

3.5. Photovoltaic parameters of QDSSCs with B-TiO_2/CdS5, B-TiO_2/CdS6, M-TiO_2/CdS5, and M-TiO_2/CdS6

Fig. 4 shows the *I–V* characteristics of QDSSCs with B-TiO_2/CdS5, B-TiO_2/CdS6, M-TiO_2/CdS5, and M-TiO_2/CdS6 as the photoanodes; the corresponding photovoltaic parameters are summarized in Table 3. The efficiencies of B-TiO_2/CdS5 and M-TiO_2/CdS5 are similar, i.e., 1.35% and 1.37%, respectively. The next SILAR cycle (6th cycle) for depositing more CdS in M-TiO_2 film has apparently

Table 2
EDX data in atomic percentage corresponding to different spots, i.e., A1, A2, and A3 in Fig. 3A; B1, B2, and B3 in Fig. 3B; C1, C2, and C3 in Fig. 3C.

Elements	(A) B-TiO_2/CdS5			(B) B-TiO_2/CdS6			(C) M-TiO_2/CdS6		
	A1	A2	A3	B1	B2	B3	C1	C2	C3
C (%)	6.20	5.81	8.48	11.68	13.40	12.81	6.42	7.89	5.95
O (%)	69.34	67.46	70.39	60.84	45.35	59.02	64.87	63.54	62.04
Na (%)	1.45	1.01	1.90	2.35	2.50	2.48	2.29	2.10	2.08
S (%)	2.22	2.51	1.53	3.57	2.99	0.40	5.49	5.60	6.14
Ti (%)	19.22	21.16	16.34	18.97	32.40	22.88	16.28	16.17	18.99
Cd (%)	1.58	2.05	1.35	2.59	3.36	2.41	4.65	4.71	4.81
Total (%)	100.01	100.00	99.99	100.00	100.00	100.00	100.00	100.01	100.01
Cd/S ratio	0.71	0.82	0.88	0.73	1.12	6.03	0.85	0.84	0.78

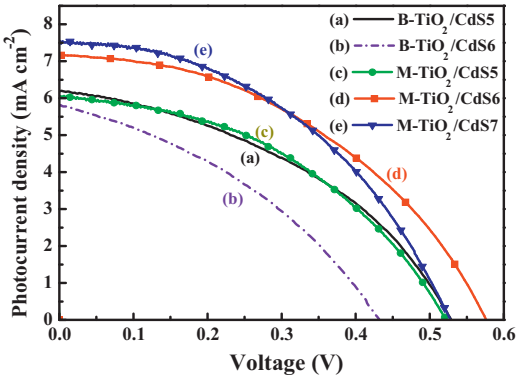

Fig. 4. Photocurrent density–voltage characteristics of QDSSCs with B-TiO_2/CdS5, B-TiO_2/CdS6, M-TiO_2/CdS5, and M-TiO_2/CdS6 as the photoanodes, measured at 100 mW cm^{-2}.

caused a dramatic difference in the structure of the film, as can be understood from the fact that there is a sudden increase in the conversion efficiency (η) in favour of the cell with M-TiO_2/CdS6 (1.79%) with reference to that of the cell with M-TiO_2/CdS5 (1.37%). Efficiency of the QDSSC with B-TiO_2/CdS6 has suddenly decreased to 0.92% from 1.35% which is the efficiency in the case of QDSSC with B-TiO_2/CdS5; that is, just one additional SILAR cycle has caused undesirable clogging of pores and resistance to ion diffusion and charge transfer and ultimately a far lesser performance to the QDSSC with B-TiO_2/CdS6. On the contrary, the efficiency of the cell using M-TiO_2/CdS6 is 1.79%. As the number of SILAR cycles is the same for both the QDSSCs with B-TiO_2/CdS6 and the M-TiO_2/CdS6, the great difference in their efficiencies is to be attributed to the modification of TiO_2 film with polystyrene in the case of M-TiO_2/CdS6 photoanode. This modification has apparently prevented unfavourable clogging of pores by CdS during its deposition, as it happened in the case of the film without modification, i.e., in the case of the film B-TiO_2/CdS6. The structural difference in the films of B-TiO_2/CdS6 and M-TiO_2/CdS6 in Fig. 3 supports this view. However, M-TiO_2/CdS7 could not render a higher efficiency to its cell than that of the cell with M-TiO_2/CdS6 (Table 3).

Table 3
Photovoltaic parameters of QDSSCs with B-TiO_2/CdS5, B-TiO_2/CdS6, and M-TiO_2/CdS obtained using 5–7 SILAR cycles for depositing CdS on them; the measurements were made at 100 mW cm^{-2}.

Photoanode films	V_{OC} (mV)	J_{SC} (mA cm^{-2})	*FF*	η (%)
B-TiO_2/CdS5	529	6.19	0.41	1.35
B-TiO_2/CdS6	431	5.82	0.37	0.92
M-TiO_2/CdS5	522	6.06	0.43	1.37
M-TiO_2/CdS6	573	7.16	0.44	1.79
M-TiO_2/CdS7	526	7.55	0.44	1.75

3.6. Correlation of EDX data with the photovoltaic performance

EDX data in Table 2 provide further explanation for the vast difference in the solar-to-electricity conversion efficiencies of the cells with B-TiO_2/CdS5 (1.35%) and B-TiO_2/CdS6 (0.92%). The quantum dots CdS, required for injecting electrons into the conduction band of TiO_2, are distributed rather in an uniform manner in the film B-TiO_2/CdS5, as can be seen from the Cd/S ratios of the film from top to bottom (Table 2). On the contrary the same quantum dots are distributed in an irregular fashion in the film B-TiO_2/CdS6, as the ratios of Cd/S in the film are quite irregular and differ by 8 times (0.73–6.03 in the film B-TiO_2/CdS6 of Table 2). This type of irregular distribution of the sensitizer (CdS) in the film cannot be expected to inject electrons efficiently into the conduction band of its TiO_2 film and can allow recombination of injected electrons with polysulfide ions in the electrolyte, as can be seen from the meagre values of J_{SC} (5.82 mA cm^{-2}) and V_{OC} (431 mV) in the case of the cell with B-TiO_2/CdS6 (Table 1). The Cd/S ratio is 6.03 in the case of the film B-TiO_2/CdS6 at the bottom of the film; this indicates the excessive Cd^{2+} at the bottom of this film; this excessive Cd^{2+} deposit could hinder the ionic diffusion and electron transfer in the film as can be seen with the meagre *FF* (0.37) for the pertinent cell (Table 1). The QDSSC with M-TiO_2/CdS6 has not only the advantages of regular porous structure for its film (Fig. 3C) as discussed above, but also a uniform distribution of CdS in its film (Table 2, case C). These two advantages probably enabled a higher ion transport and electron transfer in the M-TiO_2/CdS6 film and thereby a far superior efficiency to its cell.

3.7. Incident photon-to-current conversion efficiencies of the QDSSCs

Incident photon-to-current conversion efficiencies (IPCE) of the QDSSCs with B-TiO_2/CdS5, B-TiO_2/CdS6, and M-TiO_2/CdS6 are shown in Fig. 5. The broad IPCE curves, covering almost the entire visible spectrum from 350 to 600 nm exhibit maximum values of about 72% for the cell with M-TiO_2/CdS6, 67% for the cell with B-TiO_2/CdS5, 65% for the cell with M-TiO_2/CdS5, and 62% for the cell with B-TiO_2/CdS6; these values are in consistency with the corresponding J_{SC} values of their cells. IPCE depends on the coverage probability of CdS on TiO_2 nanocrystals and on the available space in the TiO_2 nanocrystals for light-striking. The modified porous TiO_2 structure in the case of the film M-TiO_2/CdS6, and the clogged pore structure in the case of the film B-TiO_2/CdS6 rendered IPCE values according to their structures. The IPCE value in the case of the film B-TiO_2/CdS5 has the same rationale. The large pores in the M-TiO_2 film could provide prolonged travel length for light scattering, which could enhance the IPCE value and photocurrent for the pertinent cell.

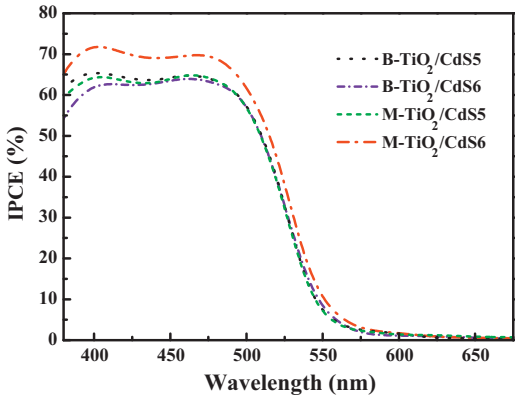

Fig. 5. IPCE spectra of the QDSSCs with B-TiO_2/CdS5, B-TiO_2/CdS6, M-TiO_2/CdS5, and M-TiO_2/CdS6.

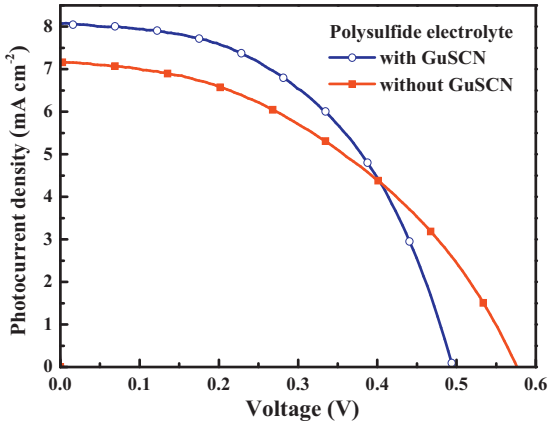

Fig. 6. Photocurrent density–voltage characteristics of the QDSSCs with the photoanode M-TiO_2/CdS6, with and without GuSCN in their electrolytes, measured at 100 mW cm^{-2}.

3.8. Photovoltaic parameters of the QDSSC with GuSCN

Based on the structure of the photoanode with M-TiO_2/CdS6, guanidine thiocyanate (GuSCN) was chosen as an additive in the electrolyte of the corresponding QDSSC; GuSCN is very well soluble in water/methanol based polysulfide electrolyte. This chemical was expecting to improve the redox rate of S^{2-}/S_x^{2-} and thereby the *FF*. Fig. 6 shows *I–V* curves of two cells both with the photoanode M-TiO_2/CdS6, however, with and without 0.1 M GuSCN in the polysulfide electrolytes of the cells. The corresponding photovoltaic parameters are listed in Table 4. Obviously, the power conversion efficiency could be enhanced from 1.79% to 2.01% (Table 4) with the addition of GuSCN in the polysulfide electrolyte of the cell with M-TiO_2/CdS6. Although the mechanism of GuSCN in the polysulfide electrolyte for improving the performance of the cell is not clear at this moment, this approach of improving the efficiency is noteworthy.

Table 4
Photovoltaic parameters of the QDSSCs with the photoanode M-TiO_2/CdS6, with and without GuSCN in their electrolytes.

Cells with M-TiO_2/CdS6	V_{OC} (mV)	J_{SC} (mA cm^{-2})	*FF*	η (%)
Without GuSCN	573	7.16	0.44	1.79
With GuSCN	498	8.07	0.50	2.01

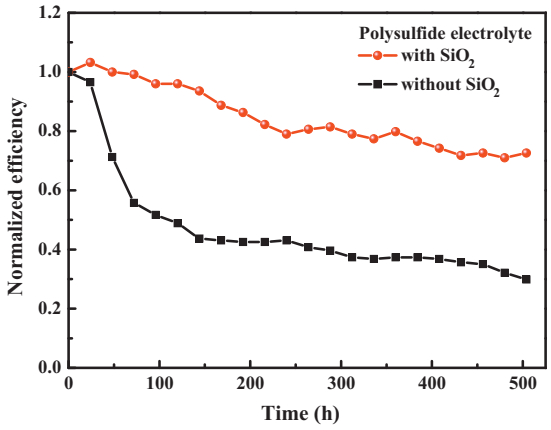

Fig. 7. The at-rest durability data of the QDSSCs with and without SiO_2 in their electrolyte.

3.9. Durability of the QDSSC

To get more information about the lifetime of the SiO_2 nanoparticels-incorporated CdS-QDSSC, we performed an experiment, measuring the cell efficiencies for more than 500 h. To our knowledge, this is the first time that such a durability test is performed for a quantum dot solar cell. Fig. 7 shows the at-rest durability data of the CdS QDSSCs with and without SiO_2 nanoparticles in their polysulfide electrolyte. All cells were sealed by surlyn® and UV glue simultaneously in this experiment. The cell efficiencies were measured once per day at room temperature. As expected, the cell with gel-like electrolyte with the incorporation of SiO_2 particles showed a much better durability compared to that of the bare one without the incorporation of SiO_2 particles. The overall power conversion efficiency of the QDSSC with SiO_2 particles has decreased by less than 30% after 500 h, while the efficiency of the other cell for the same period has decreased by more than 70%.

4. Conclusions

Polystyrene-modified TiO_2 film (M-TiO_2) with micro-cluster structure, containing micro/nano-composite pores was obtained, first by incorporating monodispersed polystyrene latex particles into the TiO_2 film and then by sintering it at 450 °C. A porous structure favourable for ion diffusion and electron transport was achieved for M-TiO_2 film. The film structure of M-TiO_2 could facilitate the assembling of well-covered, uniform CdS-QDs throughout the film; on the contrary, the bare TiO_2 film (B-TiO_2), i.e., without modification by polystyrene obtained a non-uniform deposition of CdS, as judged by the EDX data. Quantum dot-sensitized solar cells (QDSSCs) with B-TiO_2 as their photoanodes show a steady increase in their solar-to-electricity conversion efficiency with the increase of SILAR cycles from 1 to 5 for the deposition of CdS for their films; the efficiency reduces dramatically at 6th SILAR cycle. Depending on the succession of treatment of B-TiO_2 electrodes with 0.4 M Na_2S or 0.4 M $Cd(NO_3)_2$, the Cd/S ratio in the film varies between 0.71 and 6.03; the stoichiometric ratio of the quantum dots (CdS) is non-uniform in the case of the film B-TiO_2/CdS6. The M-TiO_2/CdS6 film rendered for its QDSSC an efficiency of 1.79%, compared to the efficiency of the cell with a bare TiO_2 film (B-TiO_2/CdS5, 1.37%). The QDSSC with M-TiO_2/CdS has not only the advantage of regular porous structure for its film, but also an uniform distribution of CdS in the film. IPCE values of the cells with B-TiO_2/CdS5, B-TiO_2/CdS6, and M-TiO_2/CdS6 are in consistency with the corresponding J_{SC} values and also in accordance with the respective film structures after the SILAR process. GuSCN was found to be a good additive for the

polysulfide electrolyte of a QDSSC. The additive GuSCN led to a higher efficiency (2.01%) for the QDSSC with M-TiO_2/CdS6, with reference to that of the cell with M-TiO_2/CdS6, however, without the additive. The overall power conversion efficiency of the QDSSC with SiO_2 particles has remained to be 70% of its original value after 500 h.

Acknowledgements

This work was supported in part by the National Research Council of Taiwan, under Grant numbers NSC 96-2120-M-002-016 and NSC 97-2120-M-002-012. Some of the instruments used in this study were made available through the financial support of the Academia Sinica, Taipei, Taiwan, under Grant AS-97-TP-A08.

Appendix A. Supplementary data

Supplementary data associated with this article can be found, in the online version, at doi:10.1016/j.jpowsour.2011.03.084.

References

[1] B. O'regan, M. Grätzel, Nature 353 (1991) 737–740.
[2] M. Grätzel, Inorg. Chem. 44 (2005) 6841–6851.
[3] N. Robertson, Angew. Chem. Int. Ed. 45 (2006) 2338–2345.
[4] D. Kuang, C. Klein, S. Ito, J.E. Moser, R. Humphry-Baker, N. Evans, F. Duriaux, C. Grätzel, S.M. Zakeeruddin, M. Grätzel, Adv. Mater. 19 (2007) 1133–1137.
[5] S.A. Sapp, C.M. Elliott, C. Contado, S. Caramori, C.A. Bignozzi, J. Am. Chem. Soc. 124 (2002) 11215–11222.
[6] M.K. Nazeeruddin, F.D. Angelis, S. Fantacci, A. Selloni, G. Viscardi, P. Liska, S. Ito, B. Takeru, M. Grätzel, J. Am. Chem. Soc. 127 (2005) 16835–16847.
[7] Y.L. Lee, C.H. Chang, J. Power Sources 185 (2008) 584–588.
[8] W. Lee, J. Lee, S. Lee, W. Yi, S.H. Han, B.W. Cho, Appl. Phys. Lett. 92 (2008) 153510.
[9] H. Lee, H.C. Leventis, S.J. Moon, P. Chen, S. Ito, S.A. Haque, T. Torres, F. Nüesch, T. Geiger, S.M. Zakeeruddin, M. Grätzel, M.K. Nazeeruddin, Adv. Funct. Mater. 19 (2009) 2735–2742.
[10] D.R. Baker, P.V. Kamat, Adv. Funct. Mater. 19 (2009) 805–811.
[11] M. Shalom, S. Dor, S. Rühle, L. Grinis, A. Zaban, J. Phys. Chem. C 113 (2009) 3895–3898.
[12] I. Robel, V. Subramanian, M. Kuno, P.V. Kamat, J. Am. Chem. Soc. 128 (2006) 2385–2393.
[13] L.J. Diguna, Q. Shen, J. Kobayashi, T. Toyoda, Appl. Phys. Lett. 91 (2007) 023116.
[14] S. Giménez, I. Mora-Seró, L. Macor, N. Guijarro, T. Lana-Villarreal, R. Gómez, L.J. Diguna, Q. Shen, T. Toyoda, J. Bisquert, Nanotechnology 20 (2009) 295204.
[15] L.W. Chong, H.T. Chien, Y.L. Lee, J. Power Sources 195 (2010) 5109–5113.
[16] R. Plass, S. Pelet, J. Krueger, M. Grätzel, U. Bach, J. Phys. Chem. B 106 (2002) 7578–7580.
[17] A. Zaban, O.I. Mićić, B.A. Gregg, A.J. Nozik, Langmuir 14 (1998) 3153–3156.
[18] P. Yu, K. Zhu, A.G. Norman, S. Ferrere, A.J. Frank, A.J. Nozik, J. Phys. Chem. B 110 (2006) 25451–25454.
[19] G.Y. Lan, Y.W. Lin, Y.F. Huanga, H.T. Chang, J. Mater. Chem. 17 (2007) 2661–2666.
[20] W.W. Yu, L.H. Qu, W.Z. Guo, X.G. Peng, Chem. Mater. 15 (2003) 2854–2860.
[21] L. Brus, J. Phys. Chem. 90 (1986) 2555–2560.
[22] A.J. Nozik, Chem. Phys. Lett. 457 (2008) 3–11.
[23] W. Shockley, H.J. Queisser, J. Appl. Phys. 32 (1961) 510–519.
[24] Q. Zhang, Y. Zhang, S. Huang, X. Huang, Y. Luo, Q. Meng, D. Li, Electrochem. Commun. 12 (2010) 327–330.
[25] G. Hodes, J. Phys. Chem. C 112 (2008) 17778–17787.
[26] P.V. Kamat, J. Phys. Chem. C 112 (2008) 18737–18753.
[27] O. Niitsoo, S.K. Sarkar, C. Pejoux, S. Rühle, D. Cahen, G. Hodes, J. Photochem. Photobiol. A 181 (2006) 306–313.
[28] G. Hodes, J. Manassen, D. Cahen, J. Electrochem. Soc. 127 (1980) 544–549.
[29] Y. Tachibana, H.Y. Akiyama, Y. Ohtsuka, T. Torimoto, S. Kuwabata, Chem. Lett. 36 (2007) 88–89.
[30] K.M. Lee, C.Y. Hsu, W.H. Chiu, M.C. Tsui, Y.L. Tung, S.Y. Tsai, K.C. Ho, Sol. Energy Mater. Sol. Cells 93 (2009) 2003–2007.
[31] C.P. Lee, L.Y. Lin, P.Y. Chen, R. Vittal, K.C. Ho, J. Mater. Chem. 20 (2010) 3619–3625.
[32] C.H. Chang, Y.L. Lee, Appl. Phys. Lett. 91 (2007) 053503.